Journal of Magnetic Resonance 308 (2019) 106590

Contents lists available at ScienceDirect

Journal of Magnetic Resonance

journal homepage: www.elsevier.com/locate/jmr

PE-SERF: A sensitivity-improved experiment to measure J_{HH} in crowded spectra

Chaoqun Zhan [a], Qing Zeng [a], Jinyong Chen [a], Yanqin Lin [a,b,*], Zhong Chen [a]

[a] Department of Electronic Science, Fujian Provincial Key Laboratory of Plasma and Magnetic Resonance, State Key Laboratory for Physical Chemistry of Solid Surfaces, Xiamen University, Xiamen 361005, China
[b] Shenzhen Research Institute of Xiamen University, Shenzhen 518057, China

ARTICLE INFO

Article history:
Received 28 June 2019
Revised 22 August 2019
Accepted 2 September 2019
Available online 3 September 2019

Keywords:
Nuclear magnetic resonance (NMR)
Perfect echo
Gradient-encoded selective refocusing
J-resolved
Sensitivity improvement

ABSTRACT

Aiming at facilitating the analysis of molecular structure, the gradient-encoded selective refocusing methods (G-SERF) and a great number of its variants for measuring proton-proton coupling constants have been proposed. However, the sensitivity is an issue in the 2D gradient-encoded experiments, because the signal intensity is determined by the slice thickness of the sample that depends on encoding gradient and the bandwidth of selective pulses which is limited by the smallest chemical shift difference of any two coupled protons. Here, we present a method dubbed PE-SERF (perfect echo selective refocusing) which can determine all J_{HH} values involving a selected proton with improved sensitivity compared to original G-SERF experiment. The modules of perfect echo involving selective pulses and gradient-encoded selective refocusing are combined in the method, so that the unwanted *J* couplings arising from coupled spin pairs in the same sample slice would be nullified. In this way, instead of single proton, a pair of coupled protons is allowed to share a sample slice, and thus the slice thickness can be increased and the spectral sensitivity can be improved. The performance of the method is demonstrated by experiments on quinine and strychnine.

1. Introduction

NMR spectra provide indispensable information such as scalar coupling which plays a pivotal role in molecular structure determination and analysis [1]. Unfortunately, it is often difficult to extract proton-proton scalar coupling constants since signals are often hidden in overcrowded regions in conventional 1D NMR spectroscopy. Over the last few decades, a great number of methods have been proposed to facilitate the measurement of J_{HH} values, such as *J*-resolved experiment which separates the chemical shift and scalar coupling information [2]. However, difficulties still exist in cases with crowded spectrum and signal overlap [3].

To overcome these problems, the selective refocusing (SERF) experiment, which is used to exclusively retain the J_{HH} between two selected protons, was proposed [4]. However, it needs considerably long experimental time to extract all *J* coupling constants out of a coupling network. The gradient-encoded technique was then introduced in G-SERF (gradient-encoded homonuclear selective refocusing) to improve the efficiency of the SERF experiment [5]. The principle of G-SERF is to run different selective refocusing experiments in different z-slices of the sample. Plenty of G-SERF variants have been subsequently proposed, such as real-time SERF [6] and Quick G-SERF [7] for increasing efficiency, push-G-SERF [8] for enhancing resolution and Clean G-SERF [9,10] for eradicating axial peaks. However, in these gradient-encoded experiments, the bandwidth of selective 180° pulses is determined by the closest two *J* coupled protons, and the strength of the encoding gradient is defined by the spectral width of the sample, thus limiting the thickness of the sample slices. Therefore, they have the common drawback that the spectral sensitivity is reduced by the slice-selective encoding [11]. A BSD SERF (band selective decoupled selective refocusing) was proposed to deal with the poor spectral sensitivity in the gradient-encoded experiments, while it can only be used in one special region of the spectra [12]. To avoid spatial encoding, the SECT (selective constant time) method was proposed, whose spectra must be shown in absolute-value mode [13]. In addition, SMS-SEJRES (simultaneous multi-slice selective *J*-resolved spectroscopy) was presented to simultaneously reveal all coupling networks in one experiment [14], TOCSY-edited SERF to uncover hidden resonances and afford cleaner spectra [15], and RESERF (resolution-enhanced selective refocusing) to overcome the effect of magnetic field inhomogeneity [16].

* Corresponding author at: Department of Electronic Science, Xiamen University, Xiamen, China.
E-mail address: linyq@xmu.edu.cn (Y. Lin).

https://doi.org/10.1016/j.jmr.2019.106590
1090-7807/

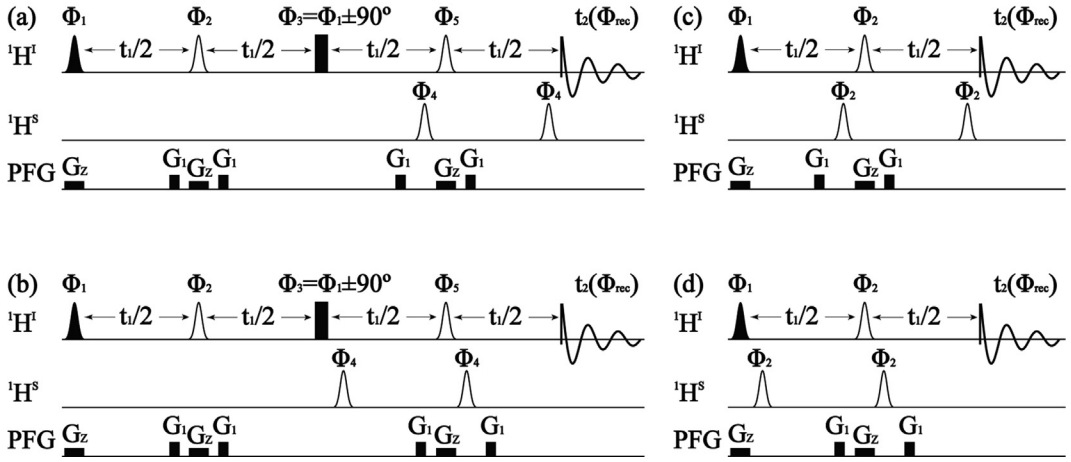

Fig. 1. The PE-SERF (a and b) and G-SERF (c and d) pulse sequences. (a) and (c) are the N-type sequences, while (b) and (d) are R-type sequences for reversed *J* spectra. Filled ellipsoidal shapes on channel $^1H^I$ represent 90° Eburp-2 shape pulses. Unfilled ellipsoidal shapes on the proton channels $^1H^I$ and $^1H^S$ are 180° Gauss or RSnob shape selective pulses. The non-encoded 180° pulses on the proton channel $^1H^S$ are applied to the selected proton S. Filled rectangles correspond to 90° hard pulse. Rectangle-shaped z-direction gradients are shown on the PFG channel. The gradient strengths are marked as G_Z and G_1. Phase cycle: Φ_1 = x, Φ_2 = x, y, −x, −y, Φ_3 = y, −y, Φ_4 = x, y, −x, −y, Φ_5 = x, Φ_{rec} = x, −x for the PE-SERF sequences in (a) and (b); Φ_1 = x, −x, x, −x, y, −y, y, −y, Φ_2 = x, x, −x, −x, y, y, −y, −y, Φ_{rec} = x, −x, x, −x, y, −y, y, −y for the G-SERF sequences in (c) and (d).

Takegoshi et al. discovered the perfect echo module that a 90° pulse is inserted at the midpoint of double spin echoes [17]. In recent years, the perfect echo module has been utilized to modify classical experiments to improve the quality of spectra [18]. PROJECT (Perfect CPMG) was presented to obtain spectra without *J* modulation in T_2 measurement [19] and PRESSIR was to obtain single voxel localized magnetic resonance spectroscopy without *J* coupling modulation [20]. The perfect echo was also used as refocusing and coherence transfer modules in CLIP-COSY [21]. Moreover, in selective experiments, including the PEPSIE (perfect echo pure shift improved experiment) [22] and perfectBASH [23,24], the perfect echo was utilized for *J* compensation. Aiming at improving the sensitivity of gradient-encoded experiments, we describe a new method entitled as PE-SERF (perfect echo selective refocusing), in which the perfect echo module involving selective pulses and gradient-encoded selective refocusing technique are employed. As the perfect echo is utilized, the *J* coupling evolution arising from the coupled spin pairs in the same sample slice would be refocused. Thus the bandwidth of selective 180° pulses increases from the smallest chemical shift difference of any two coupled protons to that of three mutually coupled protons. So that, the thickness of sample slices is allowed to be increased and sensitivity can be improved. In addition, the Pell-Keeler method [25] is used to obtain spectra with absorption-mode lineshapes. The sequences (Fig. 1a and b) with normal (N) and reversed (R) *J* evolutions acquire N- and R-type spectra, respectively. Both of obtained spectra have phase-twist lineshapes, which can be improved by summing the two spectra with one reversed along the F_1 dimension to cancel dispersive parts. Therefore, this PE-SERF experiment can improve the sensitivity, facilitating the measurement of *J* coupling constants in the analysis of molecular structure.

2. Methods

The Pell-Keeler method is used to obtain absorption-mode G-SERF spectra for fair comparison between PE-SERF and G-SERF, although the latter employed the z-filter module in the original publication [5]. Fig. 1a and b shows the N- and R-type PE-SERF sequences, and Fig. 1c and d the N- and R-type G-SERF sequences. For the PE-SERF sequences the selective 90° pulse along with a simultaneously applied weak field gradient marked as G_Z excites different spins in different z-slices of the sample, with no more than two coupled spins affected in the same z-slice. Then, in the perfect echo module, the encoded 180° selective pulses (the selective 180° pulses along with a simultaneously applied encoding gradients) are used to refocus all *J* coupling evolution on the proton channel $^1H^I$. On the proton channel $^1H^S$, non-encoded 180° selective pulses are applied to reintroduce the *J* coupling evolution involving proton S by inverting the selected proton S. For simplicity, in a coupled system composed of three protons S, I_1 and I_2, whose chemical shifts are assumed in the increasing order, the *J* coupling constants are J_{I_1S}, J_{I_2S} and $J_{I_1I_2}$. Here, we consider the z-slice of sample where protons I_1 and I_2 are excited. The non-encoded 180° selective pulses is exerted on proton S. The *J*-evolution through the N-type PE-SERF sequence are briefly described by the following analysis of product operator (see detailed analysis in the Supporting Information), while chemical shift is ignored as chemical shift evolution is refocused.

After the first selective 90° pulse, the reduced density operator $I_{1z}+I_{2z}$ turns to

$$-(I_{1y}+I_{2y}) \tag{1}$$

Then, the density operator after the first spin echo becomes

$$(I_{1y}+I_{2y})\cos\left(\pi J_{I_1I_2}t_1\right)-(2I_{1x}I_{2z}+2I_{2x}I_{1z})\sin\left(\pi J_{I_1I_2}t_1\right). \tag{2}$$

The scalar coupling evolutions between I_1 and S and between I_2 and S would both be refocused, while that between I_1 and I_2 remains unaltered. It is seen from Eq. (2) that the anti-phase magnetizations $(2I_{1x}I_{2z}+2I_{2x}I_{1z})\sin\left(\pi J_{I_1I_2}t_1\right)$ was generated after the first spin echo.

Then, the 90° pulse along *y*-axis exchanges the I_1 and I_2 anti-phase terms, while the in-phase terms $(I_{1y}+I_{2y})\cos\left(\pi J_{I_1I_2}t_1\right)$ remain unaltered. It is shown as

$$(I_{1y}+I_{2y})\cos\left(\pi J_{I_1I_2}t_1\right)+(2I_{1z}I_{2x}+2I_{2z}I_{1x})\sin\left(\pi J_{I_1I_2}t_1\right). \tag{3}$$

Through the second spin echo, the density operator turns to

$$-I_{1y}\cos\left(\pi J_{I_1S}t_1\right)-2I_{1x}S_z\sin\left(\pi J_{I_1S}t_1\right)-I_{2y}\cos\left(\pi J_{I_1S}t_1\right)-2I_{2x}S_z\sin\left(\pi J_{I_2S}t_1\right). \tag{4}$$

After the second spin echo, anti-phase terms $(2I_{1x}I_{2z}+2I_{2x}I_{1z})\sin\left(\pi J_{I_1I_2}t_1\right)$ arising from the first echo are cancelled out. So that, the unwanted scalar coupling evolution between protons I_1 and I_2 sharing the same sample slice is removed. Meanwhile, the selective 180° pulses invert spin S to reserve the *J*-coupling evolution involving spin S.

N- and R-type PE-SERF sequences are exactly the same before the second echo, and the echo and anti-echo are used in the second echo in the N- and R-type PE-SERF sequences, respectively. Hence, the evolution of R-type PE-SERF sequence can be described in the same way. The density operator before the t_2 acquisition is shown as

$$-I_{1y}\cos\left(\pi J_{I_1S}t_1\right)+2I_{1x}S_z\sin\left(\pi J_{I_1S}t_1\right)-I_{2y}\cos\left(\pi J_{I_1S}t_1\right)+2I_{2x}S_z\sin\left(\pi J_{I_2S}t_1\right). \quad (5)$$

It is seen from Eqs. (4) and (5) that both the N- and R-type PE-SERF sequences have dispersive components, which are of opposite sense. Therefore, N- and R-type spectra can be combined to obtain an absorption-mode spectrum. The processing strategy to cancel the dispersive parts of the phase-twist lineshape is to sum the N-type spectrum with the R-type spectrum reversed along the F_1 dimension. The analysis of product operator can be performed in the same way when S and I_1 are excited in the same z-slice. Signal evolution is similar to that in the G-SERF experiment when there is only one spin affected in a slice. From the product operator analysis described above, the anti-phase terms arising from a coupled spin pair that share one sample slice through the first echo of the perfect echo would be cancelled after the second echo. Hence, the bandwidth of the selective pulses along with encoding gradients are allowed to cover coupled spin pairs. Therefore, the slice thickness of sample can be thicker to obtain better sensitivity compared with original G-SERF [5]. Moreover, because the bandwidth of the selective pulses applied simultaneously with encoding gradients in PE-SERF can be wider than that in G-SERF, the PE-SERF experiment performs more excellent in crowded spectra. The performance of proposed method is demonstrated by experiments on quinine and strychnine.

3. Experimental

All experiments were performed on an Agilent (Agilent Technologies, Santa Clara, CA, USA) 500 MHz NMR System equipped with a 5 mm indirect detection probe with z-gradient at 298 K. Samples were 250 mM strychnine in $CDCl_3$ and 200 mM quinine in DMSO d_6, respectively. A home-written MATLAB program was used to process experiment data, including phase correction, Fourier transform, spectra symmetrization, and 45° rotation. Particularly, data were processed with zero-filling in both dimensions and with a sine filter applied in t_1 dimensions before two-dimensional Fourier transform. After that, R-type spectrum was reversed along the F_1 dimension and was added to N-type spectrum to give an absorption-mode spectrum.

In PE-SERF experiments on quinine, the first excitation pulse was a 51.1 ms (90 Hz bandwidth) Eburp-2 shape pulse and the strength of gradient G_Z was set to 0.65 G/cm^{-1}. They were used to excite the different spins in the different z-slices of the sample. The Gaussian pulses with duration of 17.6 ms (85 Hz bandwidth) were used for inverting proton 10 (see Fig. 2) on the proton channel $^1H^S$. The RSnob shape refocusing pulses with duration of 20.6 ms (90 Hz bandwidth) were used for encoded refocusing on the proton channel $^1H^I$. The N- and R-type PE-SERF spectra were recorded in 3 h 22 min. The same Gaussian pulses were used in the two G-SERF experiments for non-encoded inversion. A 230.0 ms (20 Hz bandwidth) Eburp-2 shape pulse in unison with a 0.65G/cm^{-1} field gradient for encoded excitation and 92.5 ms (20 Hz bandwidth) RSnob refocusing pulses on the proton channel $^1H^I$ were used in one G-SERF experiment. In order to investigate the result of G-SERF experiment with the same encoded selective pulses in PE-SERF experiment, a 51.1 ms (90 Hz bandwidth) Eburp-2 shape pulse with a 0.65 G/cm^{-1} field gradient and 20.6 ms (90 Hz bandwidth) RSnob refocusing pulses were used in the other G-SERF experiment. The N- and R-type spectra were recorded in 2 h 45 min in the first G-SERF experiment. It took 2 h 40 min to obtain N- and R-type spectra in the second G-SERF experiment. In all the experiments mentioned above, the coherence transfer pathway was selected by a pair of 9.70 G/cm^{-1} field gradient G_1 with 1 ms duration. The number of t_1 increments was set to 60 and the t_2 acquisition time was 0.8 s. Spectral width in the F_2 dimension was equal to 8 ppm and spectral width in the indirect F_1 dimension was 50 Hz. The number of scans was 64, the number of dummy scans was 32 and the recycle delay was 1 s.

For strychnine with strong coupling systems, in order to record PE-SERF spectra, the first pulse was an Eburp-2 shape pulse with

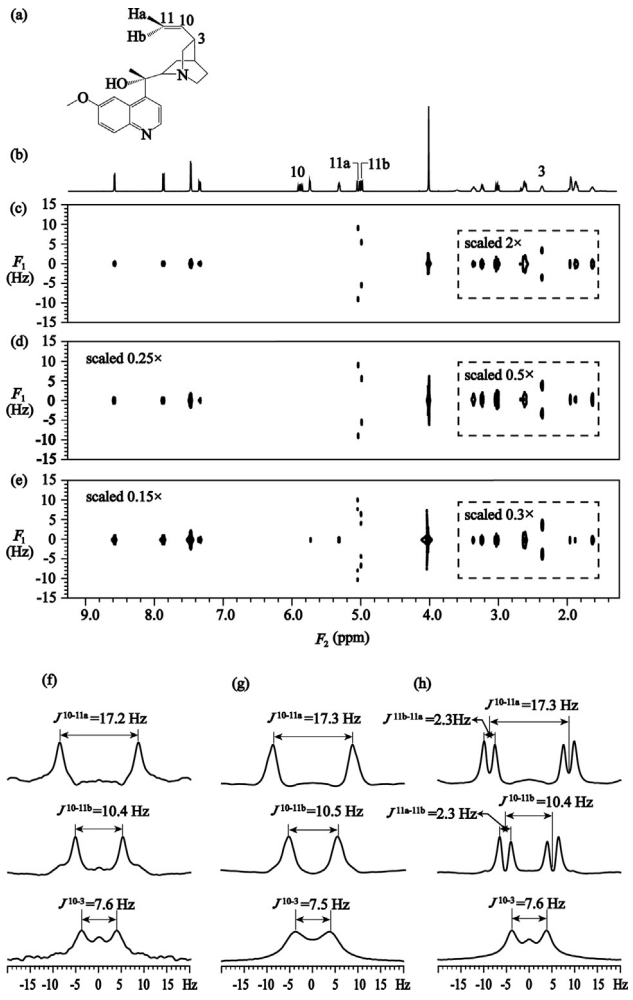

Fig. 2. Molecular structural (a) and spectra (b–h) of quinine. (b) Conventional 1D ^1H spectrum. Spectra with indicated scale factors in (c–e) show the scalar coupling networks of proton 10. (c) 2D ^1H G-SERF spectrum using 92.5 ms RSnob refocusing pulses (20 Hz bandwidth) on the proton channel $^1H^I$. (d) 2D ^1H PE-SERF spectrum using 20.6 ms RSnob refocusing pulses (90 Hz bandwidth) on the proton channel $^1H^I$. (e) 2D ^1H G-SERF spectrum using 20.6 ms RSnob refocusing pulses (90 Hz bandwidth) on the proton channel $^1H^I$. In the three experiments, the number of t_1 increments was set to 60, the number of scans was 64, the number of dummy scans was 32 and the recovery delay was 1 s. (f–h) F_1 projections of multiplets from protons 3, 11a, and 11b in the spectra in (c–e), respectively.

the duration of 66.7 ms (65 Hz bandwidth) in unison with a field gradient G_Z = 0.65 G/cm^{-1} for encoded excitation. The same encoding gradient was used together in unison with 24.0 ms (65 Hz bandwidth) Gaussian pulses for encoded refocusing. In the three experiments, 17.6 ms (85 Hz bandwidth) Gaussian pulses without encoding gradient were used to invert the protons 15b, 13 and 12, respectively, to reveal the *J* couplings involving them. Each PE-SERF spectrum was recorded in 3 h 24 min. The coherence transfer pathway was selected by a pair of 9.70 G/cm^{-1} field gradient G_1 with 1 ms duration. The number of increments along the t_1 was set to 60 and the t_2 acquisition time was 0.8 s. The F_1 and F_2 dimensions were collected with spectral widths of 8 ppm and 50 Hz, respectively. For each increment in t_1, 32 transients were acquired. The number of dummy scans was 32 and the relaxation delay was 1 s.

4. Results and discussion

The proposed PE-SERF method was first demonstrated on quinine. G-SERF and PE-SERF were used to obtain 2D *J*-edited spectra (Fig. 2c–e) which only retain the scalar couplings involving proton 10. Experimental results show three doublets corresponding to the couplings of protons 3, 11a and 11b with proton 10 in the F_1 dimension. The F_1 projections of these doublets are shown in Fig. 2f–h, respectively. The durations of encoded 180° RSnob refocusing pulses were set to 20.6 ms (90 Hz bandwidth) which covered the coupling pair 11a/11b on the proton channel $^1H^I$ in PE-SERF experiment (Fig. 2d). In contrast, because the chemical shift difference between protons 11a and 11b is 20 Hz, the bandwidth of the encoded 180° pulse should not be larger than 20 Hz (the duration of 92.5 ms) to achieve separate refocusing in G-SERF experiment (Fig. 2c). Therefore, the signal intensity would decrease in the G-SERF experiment. In the above G-SERF and PE-SERF experiments, signal-to-noise ratio (SNR) was measured on the 1D projections on the F_2 dimension. The SNR of PE-SERF spectrum was measured as 1196.7 with the noise within the range of 4.2–4.4 ppm. Meanwhile, the SNR of G-SERF spectrum was 307.4, suggesting that the PE-SERF experiment can offer superior sensitivity compared to the G-SERF experiment. The sensitivity improvement of PE-SERF spectra arises from the increase of slice thickness which is determined by the strength of the encoding gradient and the bandwidth of selective 180° pulses on the proton channel $^1H^I$ shown in Fig. 1. The PE-SERF are allowed to cover a coupled spin pair in the same sample slice so that the bandwidth of selective 180° pulses can be increased by 4.5 times in this experiment. However, the relaxation attenuation increases in the PE-SERF which contains two spin echoes, therefore the sensitivity enhancement cannot reach the theoretical value which depends linearly on the slice thickness of sample. At the same time, the durations of selective pulses in PE-SERF are shorter than those in G-SERF. This benefits the sensitivity improvement but the effect is not significant. To analyse the result when the bandwidths of selective pulses with encoding gradients cover the coupling pair 11a/11b in the G-SERF experiment, we recorded the other G-SERF spectrum employing the 20.6 ms RSnob refocusing pulses (90 Hz) on the proton channel $^1H^I$. In the Fig. 2e and h, the signal of protons 11a and 11b spilt into doublet of doublets because the bandwidth of encoded refocusing selective pulses were larger than the chemical shift difference between protons 11a and 11b and the evolution of *J* coupling between the protons 11a and 11b in the same slice of the sample cannot be refocused. The G-SERF experiment shown in Fig. 2e would lead to ambiguity in measuring the *J* coupling values involving proton 10 when the selective 180° pulses cover the coupled spin pair.

Fig. 3c is the 2D PE-SERF strychnine spectrum showing scalar coupling network corresponding to proton 15b. In the experiment,

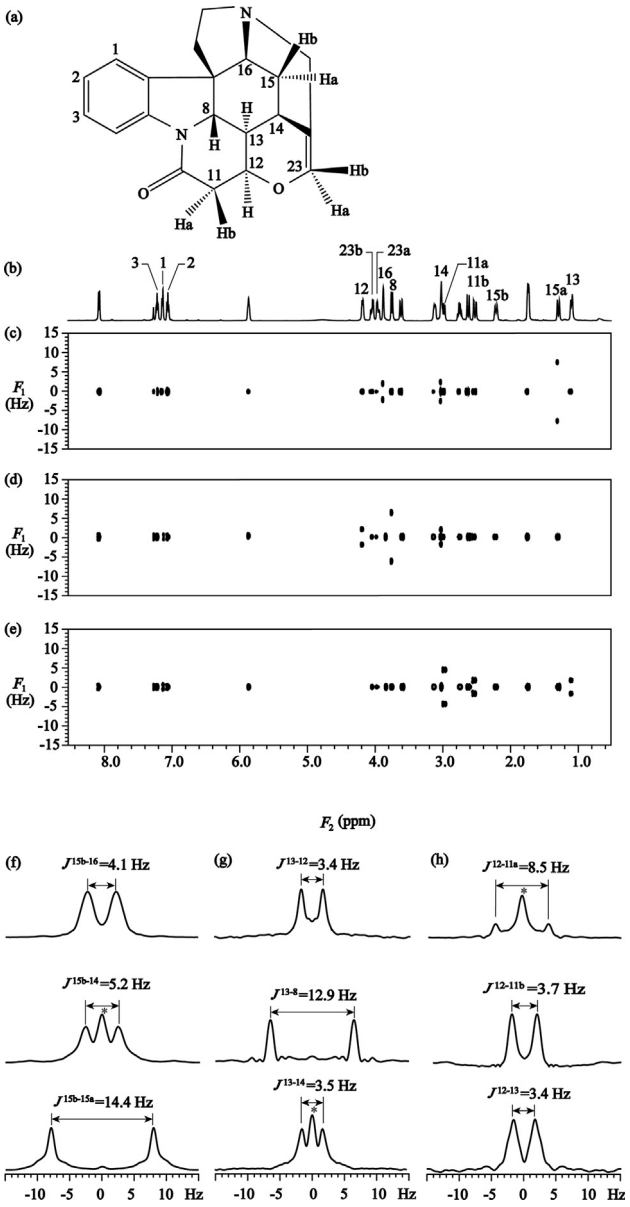

Fig. 3. (a) Molecular structural of strychnine. (b) Conventional 1D ^1H spectrum of strychnine. (c–e) The 2D ^1H PE-SERF strychnine spectra corresponding to the scalar coupling network of protons 15b, 13 and 12, respectively, using 24 ms Gaussian pulses (65 Hz bandwidth) on the proton channel $^1H^I$. In the three experiments, the number of t_1 increments was set to 60, the number of scans was 32, the number of dummy scans was 32 and the recovery delay was 1 s. (f) F_1 projections of multiplets of protons 16, 14 and 15a from spectra (c). (g) F_1 projections of multiplets of protons 12, 8 and 14 from spectra (d). (h) F_1 projections of multiplets of protons 11a, 11b, and 13 from spectra (e).

24.0 ms (65 Hz bandwidth) Gaussian pulses were used on the proton channel $^1H^I$. Proton 15b was selected by non-encoded selective 180° Gaussian pulses (17.6 ms, 85 Hz bandwidth) on the proton channel $^1H^S$, to retain scalar couplings involving the proton 15b in the indirect dimension. The *J* values involving proton 15b can be accurately measured from F_1 projections shown in Fig. 3f. The coupling networks of protons 13 and 12 are shown in Fig. 3d and e with F_1 projections in Fig. 3g and h, respectively. As chemical shifts of protons 11a and 14 are close to each other, the singlets from proton 11a marked with the asterisk appear on the F_1 projections of proton 14 in the Fig. 3f and g, and the singlet from proton 14 marked with the asterisk appears on the F_1 projection of proton 11a in Fig. 3h. The frequency differences of the strongly coupled

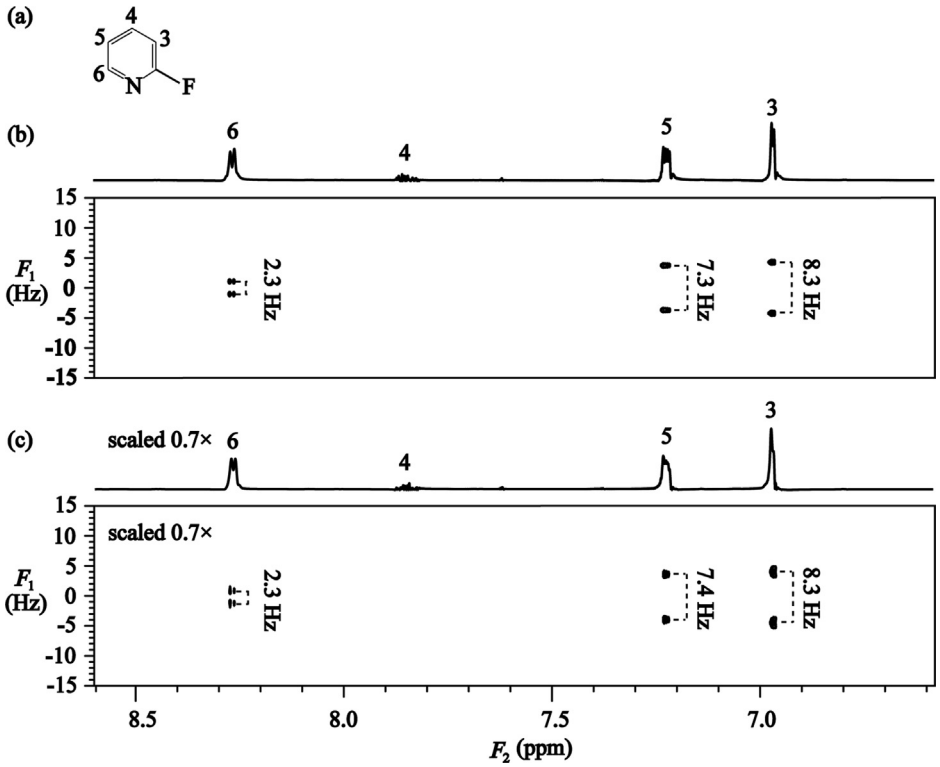

Fig. 4. (a) Molecular structural of 2-fluoropyridine. (b) 2D ^{1}H PSYCHEDELIC spectrum and its F_2 projection. (c) 2D ^{1}H PE-SERF spectrum with the indicated scale factor and its F_2 projection. 2D spectra in (b) and (c) shows the scalar coupling networks of proton 4. In both experiments, the number of t_1 increments was set to 60, the number of scans was 16, the number of dummy scans was 32 and the recovery delay was 1 s.

spin pairs 23a/23b, 2/1 and 1/3 are 45 Hz, 35 Hz and 32 Hz, respectively. In the three PE-SERF experiments, the encoded refocusing Gaussian pulses of 24.0 ms (65 Hz bandwidth) were used on the proton channel $^1H^I$, which resulted in strongly coupled proton pairs 2/1, 1/3 and 23a/23b sharing the same slice of the sample. The strong coupling effects cannot be completely eliminated, but protons 23a, 23b, 1, 2 and 3 that are not coupled to either of protons 15b, 13 and 12 show almost as singlets along the F_1 dimension. Therefore, the scalar coupling constants involving proton 15b, 13 and 12 are well measured.

Both the Pell-Keeler [25] and z-filter methods [26] can be used to obtain spectra with absorption-mode lineshape. However, the z-filter increases relaxation attenuation, halves the signal intensity, and changes the diagonally aligned multiplet pattern into square pattern. Therefore, the echo/anti-echo approach proposed in the Pell-Keeler method is adapted here to improve spectral resolution, although it needs double acquisitions.

Recently, PSYCHEDELIC [27], which is based on the PSYCHE [28] decoupling element, was proposed to measure homonuclear couplings from crowded spectra. Similar to PE-SERF experiment, PSYCHEDELIC experiment has reduced spectral sensitivity compared with conventional one, although it is based on different principle. With PSYCHE decoupling element, the sensitivity of PSYCHEDELIC spectra is proportional to $\sin^2\beta$ (β is the angle of frequency-swept chirp pulses) and is independent on chemical shift differences of protons in the spin systems. Different from PSYCHEDELIC, PE-SERF achieves selective J-evolution by using the perfect echo module and gradient-encoded selective refocusing. The bandwidths of encoded refocusing pulses, which determine the thickness of z-slices of the sample, are limited by the smallest chemical shift difference of any three coupled protons in the PE-SERF experiments. Hence, the sensitivity of PE-SERF spectra experiment depends on the specific spin systems studied. Stated otherwise, it is difficult to directly compare the sensitivity of PE-SERF with that of the PSYCHEDELIC method [27]. In some systems that the chemical shift difference of any three coupling protons is large, the PE-SERF method delivers better sensitivity than PSYCHEDELIC method, while in the other systems the latter performs more excellently. As a supplement, a sample of 200 mM 2-fluoropyridine in $CDCl_3$ was used in PSYCHEDELIC and PE-SERF experiments to compare the spectral sensitivity. The angle of frequency-swept chirp pulses was set to 15° ($\beta = 15°$) in PSYCHEDELIC experiment, and 5.5 ms (283 Hz bandwidth) Gaussian pulses on the proton channel $^1H^I$ were used in the PE-SERF experiment. The strength of gradient G_Z was 0.22 G/cm^{-1} in PSYCHE decoupling element and PE-SERF experiment. Fig. 4 shows the PSYCHEDELIC and PE-SERF spectra of 2-fluoropyridine. The SNRs for the proton 3 are 323.2 and 433.8 in PSYCHEDELIC and PE-SERF spectra, respectively. Here, the noise is calculated within the range of 1.2–1.8 ppm. In this sample, PE-SERF performs better in terms of sensitivity.

In the perfect echo module, as the 90° pulse is inserted at the midpoint of double spin echoes, the anti-phase terms introduced by the first echo can be cancelled by the second echo. It is also known that the J modulation of a coupling pair can be cancelled in case that the evolution time satisfies $t_1/2 \ll 1/\Delta\nu$ ($t_1/2$ is the interpulse spacing of spin echoes and $\Delta\nu$ is the chemical shift differences between coupled two spins) or that the spin system studied is an AX system. In the PE-SERF experiments, the evolution time t_1 of the echo needs to be increased from 0 to $\frac{1}{sw_1} * (ni\text{-}1)$ ms (sw_1 is the spectral width along F_1 dimension, ni is the number of t_1 increments), so that the condition of $t_1/2 \ll 1/\Delta\nu$ is hard to be met. Therefore, the PE-SERF experiment is only effective when the coupling pairs that share the same z-slice of the sample are AX spin systems. This type of spin system is commonly available

in molecules such as those composed of benzene rings. The PE-SERF experiment can benefit scalar coupling measurement in spin systems with such spin pairs.

5. Conclusion

In summary, we introduced a new PE-SERF experiment to measure scalar couplings constants involving a selected proton. As PE-SERF allows two coupled protons to share the same z-slice of the sample, it can improve the spectral sensitivity compared to original G-SERF. The extent of sensitivity improvement for PE-SERF is determined by the spin systems studied. The method proposed here can benefit molecular structure elucidation.

Acknowledgements

This work was partially supported by the National Natural Science Foundation of China (Grant Numbers U1732158 and U1632274), the Key Science and Technique Project of Fujian Province (Grant Number 2018Y0077), Natural Science Foundation of Guangdong Province (Grant Number 2018A030313794), and Fundamental Research Funds for the Central Universities (Grant number 20720170036).

Appendix A. Supplementary material

Supplementary data to this article can be found online at https://doi.org/10.1016/j.jmr.2019.106590.

References

[1] W.A. Thomas, Unravelling molecular structure and conformation—the modern role of coupling constants, Prog. Nucl. Magn. Reson. Spectrosc. 30 (1997) 183–207.
[2] W.P. Aue, J. Karhan, R.R. Ernst, Homonuclear broad band decoupling and two-dimensional *J*-resolved NMR spectroscopy, J. Chem. Phys. 64 (1976) 4226–4227.
[3] Y. Lin, Q. Zeng, L. Lin, Z. Chen, P.B. Barker, High-resolution methods for the measurement of scalar coupling constants, Prog. Nucl. Magn. Reson. Spectrosc. 109 (2018) 135–159.
[4] T. Facke, S. Berger, SERF, a new method for H,H spin-coupling measurement in organic chemistry, J. Magn. Reson. Series A 113 (1995) 114–116.
[5] N. Giraud, L. Beguin, J. Courtieu, D. Merlet, Nuclear magnetic resonance using a spatial frequency encoding: application to *J*-edited spectroscopy along the sample, Angew. Chem. Int. Ed. 49 (2010) 3481–3484.
[6] N. Gubensak, W.M. Fabian, K. Zangger, Disentangling scalar coupling patterns by real-time SERF NMR, Chem. Commun. 50 (2014) 12254–12257.
[7] N. Lokesh, S.R. Chaudhari, N. Suryaprakash, Quick re-introduction of selective scalar interactions in a pure-shift NMR spectrum, Chem. Commun. 50 (2014) 15597–15600.
[8] D. Pitoux, B. Plainchont, D. Merlet, Z. Hu, D. Bonnaffe, J. Farjon, N. Giraud, Fully resolved NMR correlation spectroscopy, Chem. Eur. J. 21 (2015) 9044–9047.
[9] S.K. Mishra, N. Suryaprakash, Pure shift edited ultra high resolution NMR spectrum with complete eradication of axial peaks and unwanted couplings, J. Magn. Reson. 279 (2017) 74–80.
[10] S.K. Mishra, N. Lokesh, N. Suryaprakash, Clean G-SERF an NMR experiment for the complete eradication of axial peaks and undesired couplings from the complex spectrum, RSC Adv. 7 (2017) 735–741.
[11] S. Berger, A quarter of a century of SERF: the progress of an NMR pulse sequence and its application, Prog. Nucl. Magn. Reson. Spectrosc. 108 (2018) 74–114.
[12] J.E. Herbert Pucheta, D. Pitoux, C.M. Grison, S. Robin, D. Merlet, D.J. Aitken, N. Giraud, J. Farjon, Pushing the limits of signal resolution to make coupling measurement easier, Chem. Commun. 51 (2015) 7939–7942.
[13] L. Lin, Z. Wei, Y. Lin, Z. Chen, Measuring J_{HH} values with a selective constant-time 2D NMR protocol, J. Magn. Reson. 272 (2016) 20–24.
[14] Q. Zeng, L. Lin, J. Chen, Y. Lin, P.B. Barker, Z. Chen, A simultaneous multi-slice selective *J* -resolved experiment for fully resolved scalar coupling information, J. Magn. Reson. 282 (2017) 27–31.
[15] A. Fredi, P. Nolis, T. Parella, Accurate measurement of JHH in overlapped signals by a TOCSY-edited SERF experiment, Magn. Reson. Chem. 55 (2017) 525–529.
[16] Q. Zeng, Y. Lin, Z. Chen, Pushing resolution limits for extracting ^{1}H–^{1}H scalar coupling constants by a resolution-enhanced selective refocusing method, J. Chem. Phys. 150 (2019) 184202.
[17] K. Takegoshi, K. Ogura, K. Hikichi, A perfect spin echo in a weakly homonuclear *J*-coupled two spin-12 system, J. Magn. Reson. 84 (1989) 611–615.
[18] T. Parella, Towards perfect NMR: Spin-echo versus perfect-echo building blocks, Magn. Reson. Chem. 57 (2019) 13–29.
[19] J.A. Aguilar, M. Nilsson, G. Bodenhausen, G.A. Morris, Spin echo NMR spectra without *J* modulation, Chem. Commun. 48 (2012) 811–813.
[20] Y. Lin, L. Lin, Z. Wei, J. Zhong, Z. Chen, Localized one-dimensional single voxel magnetic resonance spectroscopy without *J* coupling modulations, Magn. Reson. Med. 76 (2016) 1661–1667.
[21] M.R. Koos, G. Kummerlowe, L. Kaltschnee, C.M. Thiele, B. Luy, CLIP-COSY: a clean in-phase experiment for the rapid acquisition of COSY-type correlations, Angew. Chem. Int. Ed. 55 (2016) 7655–7659.
[22] J. Ilgen, L. Kaltschnee, C.M. Thiele, A pure shift experiment with increased sensitivity and superior performance for strongly coupled systems, J. Magn. Reson. 286 (2018) 18–29.
[23] J. Ilgen, L. Kaltschnee, C.M. Thiele, perfectBASH: band-selective homonuclear decoupling in peptides and peptidomimetics, Magn. Reson. Chem. 56 (2018) 918–933.
[24] A. Verma, S. Bhattacharya, B. Baishya, Perfecting band selective homo-decoupling for decoupling two signals coupled within the same band, RSC Adv. 8 (2018) 19990–19999.
[25] A.J. Pell, J. Keeler, Two-dimensional *J*-spectra with absorption-mode lineshapes, J. Magn. Reson. 189 (2007) 293–299.
[26] M.J. Thrippleton, J. Keeler, Elimination of zero-quantum interference in two-dimensional NMR spectra, Angew. Chem. Int. Ed. 115 (2003) 4068–4071.
[27] D. Sinnaeve, M. Foroozandeh, M. Nilsson, G.A. Morris, A general method for extracting individual coupling constants from crowded ^{1}H NMR spectra, Angew. Chem. Int. Ed. 55 (2016) 1090–1093.
[28] M. Foroozandeh, R.W. Adams, N.J. Meharry, D. Jeannerat, M. Nilsson, G.A. Morris, Ultrahigh-resolution NMR spectroscopy, Angew. Chem. Int. Ed. 53 (2014) 6990–6992.